Real Time Detection of Lysozyme by Pulsed Streaming Potentials Using Polyclonal Antibodies Immobilized on a Renewable Nonfouling Surface Inside Plastic Microfluidic Channels

ARTICLE *in* ANALYTICAL CHEMISTRY · FEBRUARY 2011

Impact Factor: 5.64 · DOI: 10.1021/ac102769j · Source: PubMed

3 AUTHORS, INCLUDING:

Fernando Luna Vera
Centro Nacional de asistencia técnica a la In…
4 PUBLICATIONS **36** CITATIONS
SEE PROFILE

Julio C Alvarez
Virginia Commonwealth University
15 PUBLICATIONS **156** CITATIONS
SEE PROFILE

analytical chemistry

ARTICLE

pubs.acs.org/ac

Real Time Detection of Lysozyme by Pulsed Streaming Potentials Using Polyclonal Antibodies Immobilized on a Renewable Nonfouling Surface Inside Plastic Microfluidic Channels

Fernando Luna-Vera,[†] Josephus D. Ferguson,[‡] and Julio C. Alvarez*[,†]

[†]Department of Chemistry, Virginia Commonwealth University, P.O. Box 842006, Richmond, Virginia 23284, United States

[‡]Department of Physics, Virginia Commonwealth University, Richmond, Virginia 23284, United States

Supporting Information

ABSTRACT: A composite surface was prepared on cyclic olefin copolymer (COC) microchannels by UV-photografting of polyethylene glycol acrylate (PEGA) and poly(acrylic acid) (PAA) films. A PEGA layer of globular particles with average thickness of 60 nm was formed after 15 min of polymerization. Real time monitoring by pulsed streaming potentials demonstrated the ability of the PEGA layer to inhibit the adhesion of five different nonspecific adsorbing proteins when compared with pristine COC. Roughness determined by atomic force microscopy (AFM) after PAA grafting on COC-PEGA at different UV illumination times suggests that PAA formation is initiated at the free space in between the PEGA particles. Carboxylic groups activated with *N*-hydroxysuccinimide and *N*-ethyl-*N*′-(3-dimethylaminopropyl) carbodiimide were used to bind anti-lysozyme polyclonal antibodies. The composite COC-PEGA-PAA-anti-lysozyme surface demonstrated its ability to detect lysozyme with a dynamic range between 140 and 860 nM. Linearity was maintained even when samples were spiked with 250 nM of cytochrome as interfering species. The equilibrium constant K_{eq} for the adsorption of Ly on COC-PEGA-PAA-anti-Ly was estimated to be $2.7 \times 10^6\ M^{-1}$, and it shows that this kinetic approach of monitoring the surface charge is also useful to estimate affinity interactions for proteins in label free fashion. The regeneration of the surface exhibited an average percentage of recovery of ~97% for each of six adsorption−regeneration cycles. This feature enables curve calibration on a single microfluidic chip because each point of the curve has a reproducible and renewable surface.

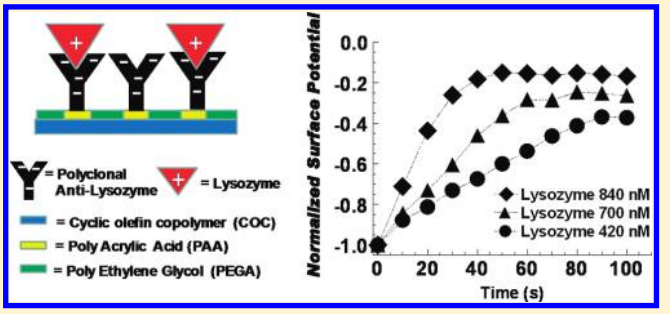

Herein we report the preparation of a hydrophilic composite surface by UV-photografting of poly(ethylene glycol acrylate) (PEGA) and poly(acrylic acid) (PAA) films on microchannels fabricated with the plastic cyclic olefin copolymer (COC).[1] This surface modification allows the easy regeneration of the surface ζ potential, which in turn enables consecutive and reproducible detection of protein adsorption in real time by pulsed streaming potentials. Streaming potentials are spontaneous ion gradients created when solutions move through microchannels by pressure-driven flow.[2−4] At the microscopic interface between the liquid and the surface, the forward liquid flow creates a downstream excess of surface counterions which is manifested as a potential difference along the flow axis and can be detected by two electrodes located at the outlets of the microchannel.[2−4] The polarity and magnitude of the measured potential, which can be used to monitor and detect adsorption processes, is related to the liquid pressure and the ζ potential of the microchannel surface.[2−4] Previously, we have implemented this principle in COC microfluidic channels for the detection of heparin employing pulsated liquid flow which allowed the use of nonreference electrodes with no compromise in the precision of equilibrium measurements of pulsed streaming potentials.[2] We have also reported a new strategy for sample introduction which allows the kinetic measurement of lysozyme (Ly) adsorption in real time on COC.[3] One problem revealed by these kinetic studies was the nonspecific adsorption that prevented regeneration of the original surface charge and made difficult consecutive reproducible measurements using the same microfluidic channel.[3] Also, because these adsorption kinetic studies were performed on pristine COC, the Ly detection did not have any selectivity.[3] Herein we address these problems by preparing a composite hydrophilic film which provides a renewable nonfouling surface and at the same time imparts some degree of specificity by allowing the linkage of Anti-Ly polyclonal antibodies. Furthermore, we used the kinetic monitoring of the surface charge by pulsed streaming potentials to optimize the preparation of the composite film as well as to assess its selectivity and sensitivity. The main significance of this work relies on

Received: October 21, 2010
Accepted: January 22, 2011

having developed a surface detection technique of general applicability that does not require chemical labeling but provides significant mitigation of nonspecific adsorption while still providing nanomolar detection limits with some degree of specificity for Ly. Lysozyme is an enzyme that helps natural protection against pathogens and is present in body secretions such as saliva, mucus, and tears.[5] Herein Ly is used as a model for developing a protein sensor using pulsed streaming potentials, but because binding constants can be obtained, it is also a model for studying protein interactions with immobilized probes.

The understanding of protein interactions like those occurring in protein−peptide binding,[6] pathogen−host interactions,[7] and amyloid formation[8] is very important to determine biological function and physiological health. Surface based techniques such as surface plasmon resonance (SPR), quartz crystal microbalance (QCM), and pulsed streaming potentials (PSP) are very suitable for such studies because these techniques do not require chemical labeling and allow surface immobilization of one of the targets in the interaction. The approach by streaming potentials is unique because it is the only one that responds to variations in the surface charge and also allows kinetic monitoring of the adsorption processes.[3] The surface confinement present in these techniques can better mimic the congregation environment that cellular organelles and membrane macromolecules provide in vivo as opposed to studying interactions in the bulk.[9] Nonetheless, the investigation of interactions between solution species and immobilized targets on surfaces is difficult because nonspecific adsorption (NSA) can obscure the signal of binding events. In hydrophobic substrates, like COC and bare gold, adsorption of proteins occurs spontaneously and is responsible in great part for the NSA and the irreversible fouling observed in such surfaces.[10−12] The challenge for creating platforms to study surface−probe interactions (or surface based sensors) consists in preventing NSA but at the same time providing surface receptors with good specificity. This would improve the sensing performance of the surface and in some cases reduce the cost of analysis by allowing surface regeneration. The immobilization of hydrophilic and nonionizable films has been the main strategy to circumvent NSA. Approaches such as the immobilization of hydrogels like carboxymethyl dextran has been used on the metallic surface of SPR chips.[13] However, poly(ethylene glycol) is probably the most widely used material to prevent NSA and has been immobilized on almost every surface including silicon,[14] poly(methyl methacrylate),[15] glass,[16] and gold.[17]

In this paper, we describe the surface modification of hydrophobic COC microchannels by sequential photografting of poly(ethylene glycol acrylate) and poly(acrylic acid) to provide nonfouling properties. The attachment of polyclonal anti-Ly was performed to impart some specificity for the adsorption and detection of Ly. Structural and morphological characterization of the composite surface was done by atomic force microscopy (AFM) and FT-IR. Selectivity and fouling evaluation was done with four additional proteins and using cytochrome as the interfering species.

EXPERIMENTAL SECTION

Chemicals. Double crystallized and dialyzed lysozyme was purchased from Worthington Biochemical Corporation (Lakewood, NJ). NaCl 99.5%, NaH_2PO_4, and Na_2HPO_4 were obtained from Merck (San Diego, CA). Cytochrome C from horse heart (CYT), Fibrinogen fraction I from human plasma (FIB), albumin from human serum 97−99% (HSA), bovine serum albumin (BSA), poly(ethylene glycol acrylate) (PEGA), 2-(*N*-morpholino) ethanesulfonic acid (MES), *N*-hydroxysuccinimide (NHS), *N*-ethyl-*N*′-(3-dimethylaminopropyl)carbodiimide (EDC), and acrylic acid anhydrous (AA) were products from Sigma (St. Louis, MO). Rabbit polyclonal antibody to lysozyme (Ly) was obtained from AbCam (Cambridge, MA).

Surface Characterization.

$$E = \frac{P\zeta\varepsilon\varepsilon_\circ}{\eta\kappa} \quad (1)$$

The streaming potential (E), which is proportional to the liquid pressure, was recorded at different pH for pristine COC and COC-PEGA microchannels and then plugged into the Smoluchowski equation (eq 1) to calculate the ζ potential.[2−4] The ζ potential is defined as the potential at the slippage plane of the liquid, but it can be considered as the surface charge.[4] Equation 1 also includes parameters such as the solution viscosity (η), conductivity (κ), vacuum permittivity (ε_o), and dielectric constant (ε), which contribute to the value of E; however, changes in those contributions can be minimized by working with dilute solutions. Phosphate buffer solutions of approximately 1.5 mM from pH 2.3 to 10.7 and a constant conductivity of 389 ± 4 μS cm^{-1} were used to record E. Each solution was pumped into the microchannels using 10 pulses of 1 s and their average reported as a single value. The viscosity and dielectric constant used for the calculation were those for pure water at 20 °C.

Spectroscopic characterization of the composite film was performed by attenuated total reflectance Fourier transform-infrared (ATR FT-IR) of modified COC open plates. PEGA was grafted on a COC plate by covering the surface with a solution of 15% monomer and 0.2% benzophenone and then applying UV illumination for 15 min. Subsequently, AA was polymerized using 15% of monomer and 0.2% benzophenone with 15 min of UV irradiation. The carboxylate groups in the PAA layer were used to attach polyclonal anti Ly using 0.4 M EDC and 0.1 M NHS in 0.1 M MES buffer pH 5.1. After each step, the surface was toughly washed with water and PBS 1× and spectroscopically analyzed by ATR-FT-IR on a Nicolet Nexus 870-FTIR spectrometer using 200 scans with 4 cm^{-1} of resolution. An Avatar Multi-Bounce HATR accessory was used for this purpose, and the crystal was ZnSe with an incidence angle of 45°. The different surfaces denoted as COC, COC-PEGA, COC-PEGA-PAA, and COC-PEGA-PAA-anti-Ly were also analyzed by AFM in tapping mode employing a Veeco ICON dimension instrument.

Sensor Response to Lysozyme and Cytochrome As Interfering Species. The ability of the COC-PEGA-PAA-anti-Ly microchannels to generate a reproducible and linear response toward Ly with and without interfering species was evaluated using cytochrome (CYT). Solutions of Ly in the range of 0.0−840 nM were prepared, and each concentration sample was introduced in the channel using a series of 5 pulses of 1 s each (no still time between each series) during 100 s. Protein-free buffer was flowed under the same conditions during 100 s before introduction of the samples. The average streaming potential of five consecutive pulses was divided by the streaming potential value obtained with protein-free buffer and reported as a corrected normalized streaming potential Ec.[3] After adsorption of each protein solution, the surface was regenerated by flowing

dx.doi.org/10.1021/ac102769j |*Anal. Chem.* XXXX, XXX, 000–000

Scheme 1. Sequence of Steps for the Production of a Nonfouling Surface with Some Selectivity for Ly

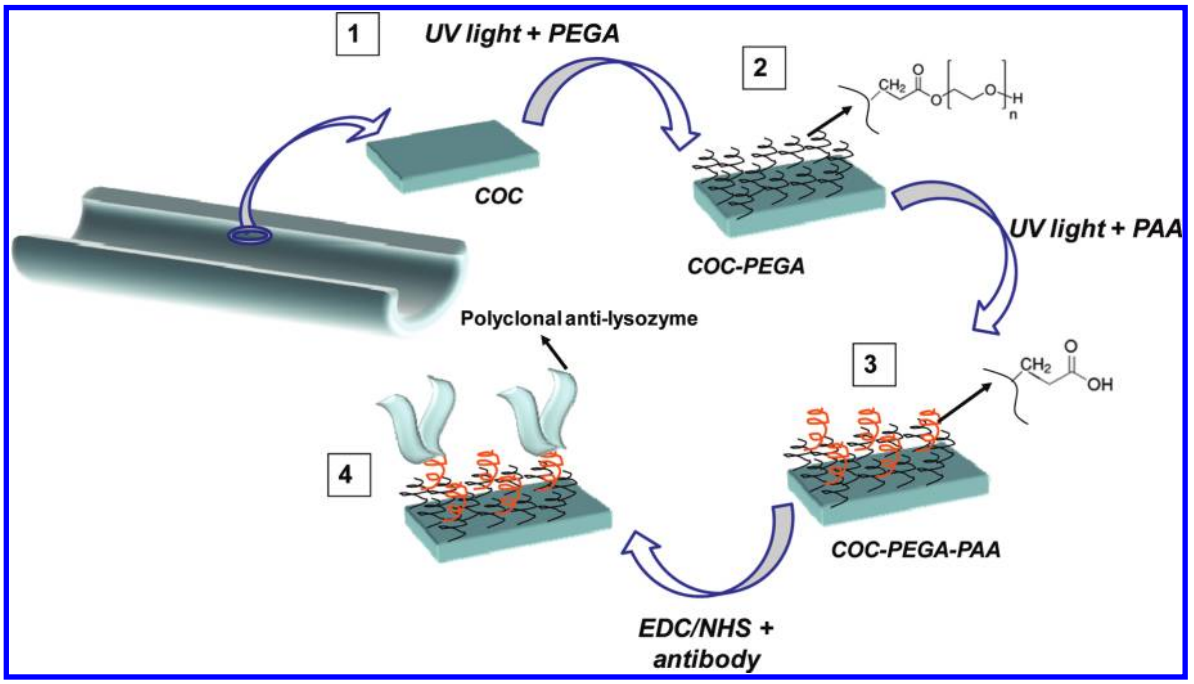

NaCl 0.5 M during 300 s and used for the adsorption of the next sample. A second series of samples with the same concentration of Ly but containing 250 nM of CYT were analyzed in three independent chips using the same pulse conditions. Values of the slope (dEc/dt) determined from the linear region (first 30 s) of adsorption isotherms Ec vs t per each concentration were used to prepare calibration curves by plotting (dEc/dt vs [Ly]).[3] All solutions were prepared in phosphate buffer 1.5 mM pH 7.1 and 258 μs cm^{-1}. Details of the photopolymerization of PEGA and PAA on COC as well as the nonspecific adsorption experiments for proteins are described in the Supporting Information.

RESULTS AND DISCUSSION

Preparation, Optimization, and Characterization of the Microchannel Surface. The goal of this research was to modify the COC microchannel surface with a composite film that could provide both nonfouling properties and selective receptors for binding Ly. This approach is a model for protein sensors based on pulsed streaming potentials. However it is also a model of a platform for studying protein interactions with immobilized probes, given the fact that this detection technique allows kinetic monitoring of surface adsorption with no need for chemical labeling for the targets under study. To this end, the procedure depicted in Scheme 1 was devised, first a layer of PEGA was UV-photografted on COC to produce COC-PEGA and then PAA was photopolymerized on top (COC-PEGA-PAA) to provide anchoring groups for the antibody receptors. The last step consisted of attaching the polyclonal antibodies (anti-Ly) on the activated carboxylate groups of PAA (COC-PGA-PAA-anti-Ly). Characterization by pulsed streaming potentials, AFM tapping mode, and ATR-FTIR was performed at the various steps.

Figure 1A shows the ζ potential for COC-PEGA, COC-PEGA-PAA-anti-Ly, and pristine COC illustrating the decrease in the value of ζ as function of the pH observed in the range 3.4−10.7. For instance, at pH 3.4 the ζ value for COC-PEGA is ∼0.0 mV and it decreases gradually to −15 mV when increasing the pH to 10.7. For COC-PEGA-PAA-anti-Ly, the ζ potential decreases from ∼+15 to −30 mV in the same range of pH which is consistent with the incorporation of negatively charged carboxylate groups from PAA. On the other hand, COC has a ζ value of +10 mV at pH 3.4, and it reaches a value of −65 mV at pH 10.7. This behavior has been reported before, and it has been attributed to anion adsorption, presumably hydroxide ions.[18] Therefore, the smaller variation in ζ observed for COC-PEGA as a function of pH (∼15 mV) compared to pristine COC (∼70 mV) is seemingly indicative of the lower tendency of PEGA for nonspecific adsorption of anions likely due the nonionic and hydrophilic character of the PEGA film. This change in ζ potential observed after PEGA immobilization on COC can be analyzed by estimating the charge density for both COC and COC-PEGA using the Gouy−Chapman relationship (eq 2).[19] The charge density is represented by σ, ε_o is the vacuum permittivity, ε is the dielectric constant, R is the gas constant (8.31 J mol^{-1} K^{-1}), T is the temperature (293 K), c it the bulk electrolyte concentration (mol L^{-1}), z is ion charge (+1), F is the Faraday constant (9.6 × 104 C mol^{-1}), and ζ is the zeta potential.

$$\sigma = \sqrt{2\varepsilon\varepsilon_{\circ}RTc}\,\sinh(zF\zeta/2RT) \qquad (2)$$

Values of charge density estimated using the ζ potential at pH 7.1 show a change from 7.12 × 10^{-5} C cm^{-2} for pristine COC to 10.6 × 10^{-6} C cm^{-2} after modification with PEGA. Assuming that this difference in σ is caused by anions of unit charge (1.6 × 10^{-19} C), this change corresponds to 3.78 × 10^{14} ions cm^{-2} or 6.28 × 10^{-10} mol ion cm^{-2}, which indicates that the PEGA film is able to reduce anion adsorption in an amount equivalent to approximately one densely packed monolayer. The typical surface density at maximum coverage for self-assembled monolayers

dx.doi.org/10.1021/ac102769j |*Anal. Chem.* XXXX, XXX, 000–000

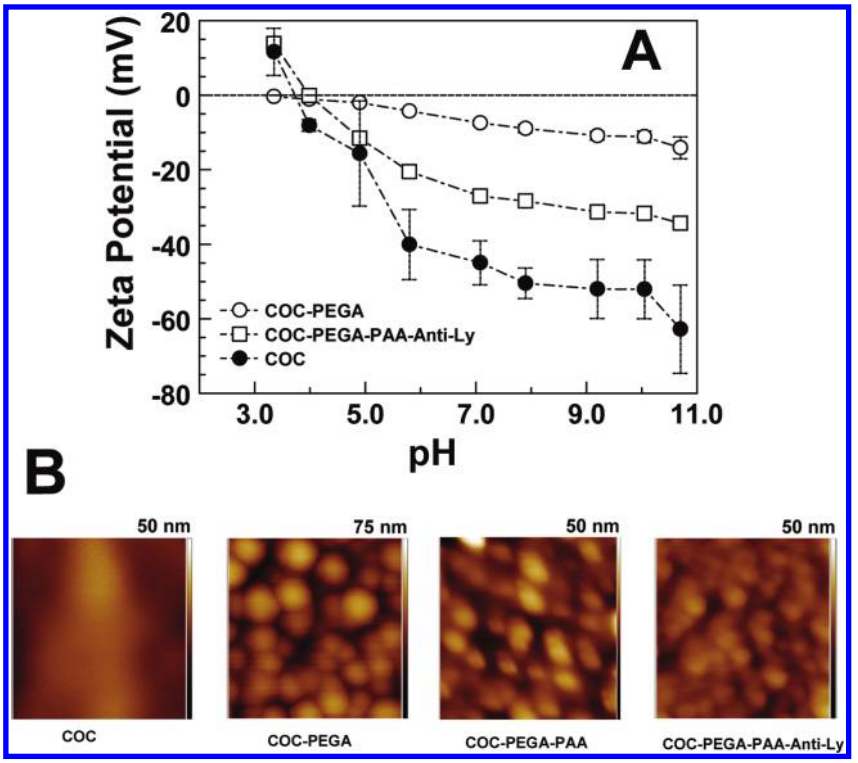

Figure 1. Comparison between COC, COC-PEGA, COC-PEGA-PAA, and COC-PEGA-PAA-anti-Ly: (A) ζ potential as a function of pH using phosphate buffer solutions between 1.5 and 2.0 mM and 389 $\pm$ 4 μS cm^{-1}. (B) Topographic AFM tapping mode images (500 nm $\times$ 500 nm). The vertical color bar represents height. For COC-PEGA-PAA, 2 min of UV illumination were used for PAA grafting.

of alkanethiols on gold has been reported to be ~4.5 $\times$ 10^{14} molecules cm^{-2}.[20]

Figure 1B shows the AFM images in tapping mode for COC, COC-PEGA, COC-PEGA-PAA, and COC-PEGA-PAA-anti-Ly. The mean square roughness (Rq) determined for COC was 4.15 nm, which increased to 7.15 nm after PEGA modification; however, after 2 min of UV induced polymerization to produce COC-PEGA-PAA, the roughness value became ~4.5 nm. This reaction time for PAA modification was the one that produced the best results for Ly adsorption (see below) and it is probably indicative of the similarity in topography between COC-PEGA-PAA and COC-PEGA-PAA-anti-Ly (Figure 1B). The morphology of the PEGA film observed is congruent with previous reports where grafted polymers described as a polymer brush adopt globular-like structure in their dry state.[21−23] The thickness of the PEGA film determined using a linear AFM scan between a COC-PEGA region and a pristine COC was found to be 66.2 $\pm$ 11.9 nm. This value was used to estimate the grafting density (σ_g) using eq 3,[24] where h is brush thickness; ρ is bulk density of the brush composition, N_a is Avogadro's number, and M_n is the number-average molecular weight.

$$\sigma_g = \frac{(h\rho N_a)}{M_n} \quad (3)$$

With the use of the ρ value of 1.18 g/cm^3 previously reported for PEGA[25] and a molecular weight of M_n = 375 g mol^{-1}, the graft density was estimated to be 1.3 $\times$ 10^2 monomer molecules nm^{-2}. This high amount of monomer molecules per area can be explained by the long time of irradiation used and the formation of hyperbranched structures during the polymerization.[26,27] Figure S1 (Supporting Information) shows a series of FT-IR spectra at different stages of modification in comparison with the spectrum for pristine COC (Figure S1A in the Supporting Information), which shows the expected bands for a purely hydrocarbon based polymer.[1] Figure S1B in the Supporting Information shows the spectrum for a COC-PEGA surface with the appearance of the C−O ether stretch band at 1095 cm^{-1} and the C═O stretch band produced by the carboxylic acid in the acryl group at 1720 cm^{-1}.[28,29] When PAA is grafted on COC-PEGA (Figure S1C in the Supporting Information), the band for C═O is still maintained but becomes broader, consistent with an additional source of carboxylate functionalities. The amide groups added when the polyclonal antibodies are attached to produce COC-PGA-PAA-anti-Ly (Figure S1D in the Supporting Information) give rise to the amide bands I and II at 1550 and 1650 cm^{-1}, respectively, as well as the N−H stretch at 3390 cm^{-1}.[30]

To determine the effect of PEGA in reducing nonspecific adsorption of proteins, COC and COC-PEGA microchannels were evaluated by pulsed streaming potentials using five proteins of different sizes and isoelectric points (pI): lysozyme (Ly), cytochrome (CYT), fibrinogen (FIB), human serum albumin (HSA), and bovine serum albumin (BSA). Figure 2 shows the adsorption and desorption phases for FIB and Ly on COC and COC-PEGA. Profiles for the other proteins are shown in Figure S2 (Supporting Information). Initially, the microchannels were flowed with protein-free solution for 300 s followed by an injection of the protein solution to monitor adsorption during 600 s. At 900 s, another injection of protein-free solution was made to follow desorption. Both FIB and Ly show very low adsorption on COC-PEGA as evidenced by the smaller change in the streaming potential (E) in comparison to bare COC. The change in E for both COC and COC-PEGA occurs in the same direction though, that is, reducing the negative surface charge of

dx.doi.org/10.1021/ac102769j |Anal. Chem. XXXX, XXX, 000–000

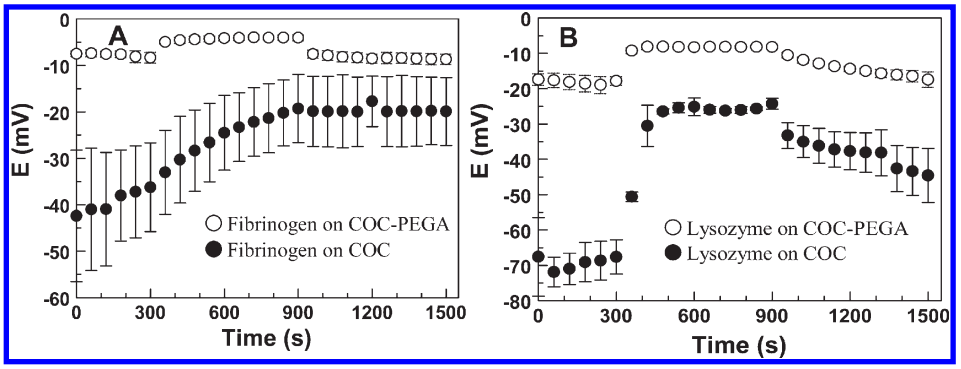

Figure 2. Kinetics of adsorption−desorption for (A) FIB and (B) Ly. Protein-free buffer, phosphate 1.5 mM, pH 7.1, and 389 ± 3 μS cm^{-1} was injected at 0 s and flowed during 300 s. At 300 s, protein solution 3 μg mL^{-1} in phosphate buffer 1.5 mM, pH 7.1, and 389 ± 3 μS cm^{-1} was injected and flowed for 600 s. At 900 s, protein-free buffer was injected again until 1500 s. For fibrinogen, protein solutions and free-protein buffer were 747 μS cm^{-1}.

Scheme 2. Model for the Reduction of Negative Charge by Nonspecific Adsorption of (A) a Positively Charged Protein and (B) a Negatively Charged Protein with Counterion Condensation

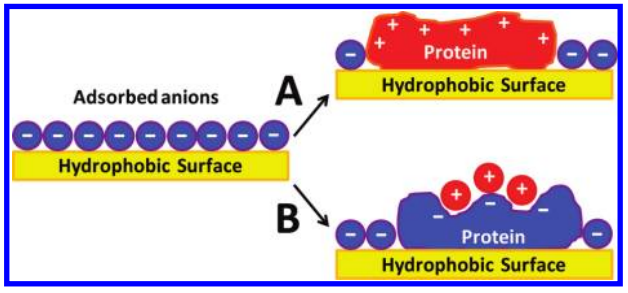

the microchannel upon nonspecific adsorption of FIB and Ly[3] as well as the other proteins (Figure S2, Supporting Information).

The magnitude of E and ζ is determined by the average surface charge density (eqs 1 and 2) inside the microchannels. Therefore, the time dependent behavior of E and ζ depends on the charge density prior to any adsorption and any concomitant change in the charge density as species adsorb on the surface. We propose that the reduction of negative charge density (less negative charge on the surface) can occur through two different mechanisms (Scheme 2) (A) adsorption of a protein with an effective positive charge that simply replaces the negative charge on the surface and (B) adsorption of a protein with an effective negative charge which is lower than the charge of the anions being replaced on the surface. Proteins contain local regions of high charge density that generate counterion condensation on those local places (Scheme 2B).[31] Condensed counterions do not contribute to the effective charge because they compensate local charge in the protein and are tightly bound making the net charge of the protein lower than the effective charge.[31] For instance, the net charge of BSA at pH 6.8 is −11.0 but it decreases to −8.4 ± 0.4 because of counterion condensation.[32] Counterions condense when the charge to charge distance within the macromolecule is smaller than the Bjerrum length which is 0.71 nm for water and it increases with the ionic strength.[33] It is conceivable that for Ly and CYT, which have pIs of 11.0 and 10.5, respectively (Table 1), follow the mechanism in Scheme 2A because they carry an effective positive charge at pH 7.1. On the other hand, FIB, HSA, and BSA, which have pI values of 5.8, 4.7, and 4.7, respectively, carry a negative charge at pH 7.1 and

Table 1. Protein Parameters and Nonspecific Adsorption on COC and COC-PEGA

			ΔE_{a-d} (mV)	
protein	molecular weight (kDa)	pI	COC	COC-PEGA
Ly	14.7	11.0	39.5 ± 12.1	0.4 ± 1.8
CYT	12.0	10.5	23.1 ± 6.6	0.5 ± 0.1
FIB	34.2	5.8	16.3 ± 2.9	−0.3 ± 0.1
HSA	66.7	4.7	11.7 ± 5.1	−0.8 ± 2.2
BSA	66.0	4.7	12.1 ± 3.8	−0.4 ± 0.9

therefore the mechanism in Scheme 2B is likely to be operative. By the same token, because the negative proteins FIB, HSA, and BSA are relatively big as indicated by their molecular weight, they provide more room for counterion condensation. For instance the dimensions of BSA are 14 × 4.0 × 4.0 nm[3],[34] which easily allows the Bjerumm length condition. Another important result from Figure 2 and Figure S2 (Supporting Information) is that after adsorption of the proteins on pristine COC, the original surface charge was never recovered because of irreversible adsorption of the proteins. In contrast, COC-PEGA showed quite renewable behavior of the surface charge under the same conditions of fouling. In order to compare the extent of nonspecific adsorption between COC and COC-PEGA, the difference in streaming potential between the beginning of the adsorption phase and the end of the desorption phase, ΔE_{a-d}, was determined (Table 1). The smaller the value of ΔE_{a-d}, the less nonspecific adsorption occurs and the more renewable the surface becomes. For all the proteins on COC-PEGA, the magnitude of ΔE_{a-d} was in the submilivolts range, whereas for COC, ΔE_{a-d} varied from 12 to 40 mV. This behavior is attributed to the nonionic and hydrophilic character of COC-PEGA, which provides an efficient blocking of the hydrophobic COC surface significantly mitigating nonspecific adsorption.

In order to detect Ly using COC-PEGA, functional groups for anchoring the Ly antibodies have to be attached. To this end, carboxylic functionalities were incorporated by photografting AA directly on the COC-PEGA microchannel surface following steps 2 and 3 in Scheme 1. Carboxylates were selected because they are well-known to be readily activated with EDC/NHS chemistry.[35] Figure S3 (Supporting Information) shows three representative AFM topographies at 0, 2, and 15 min of AA UV-initiated polymerization. The roughness Rq changes from 8.8

dx.doi.org/10.1021/ac102769j |Anal. Chem. XXXX, XXX, 000–000

nm, when no PAA is grafted, to 53.8 nm after 15 min of polymerization. Interestingly, for 2 min of illumination the roughness becomes smaller in magnitude (4.5 nm) than for the original COC-PEGA surface. This result is interpreted as an indication that the initial polymerization of PAA is presumably occurring in the pinholes of the globular PEGA film, creating a smoother surface. As a consequence, reduction in the height of the globular structures of the PEGA film from ~20 to 10 nm was observed (Figure S4A,B, Supporting Information). When the polymerization time was 15 min, PAA seems to grow over the COC-PEGA generating a rougher surface with features that reach up to 150 nm in height (Figure S4C, Supporting Information).

To establish which PAA polymerization time produces the best surface for Ly detection, Ly antibodies (anti-Ly) were attached to the COC-PEGA-PAA microchannel after activation of the carboxylic groups (Scheme 1). The time dependent variation (dEc/dt) of the corrected and normalized streaming potential Ec (see the Experimental Section), which can be considered as the initial adsorption rate of Ly, was used as a criterion to evaluate Ly adsorption on COC-PEGA-PAA-anti-Ly. Figure S5 (Supporting Information) shows values of dEc/dt at the different times of PAA polymerization. The highest adsorption rate for Ly was observed when PAA was polymerized during 2 min whereas shorter or longer times (up to 19 min) did not improve Ly detection implying that a higher number of carboxylate groups for anchoring the antibody receptors does not guarantee better detection of Ly. This could mean that at longer polymerization times, the adsorption of the protein probes is compromised by steric crowding effects of the receptors[36,37] or by an increased heterogeneity of the film.[38,39] Such increased heterogeneity was observed by AFM on the films polymerized for more than 5 min (Figure S3, Supporting Information).

Analytical Figures of Merit and Ly−Antibody Interaction. Figure 3A shows the corrected and normalized pulsed streaming potential (Ec) vs time for different concentrations of Ly adsorbed on COC-PEGA-PAA-anti-Ly. The kinetics of absorption reveals that variations of Ec with time are concentration dependent and a higher concentration of Ly produce faster adsorption rates.[3] Also the linearity of the adsorption rate (dEc/dt) as function of [Ly] (Figure 3 B) indicates that the Ly adsorption is limited by mass transport at the initial stages of adsorption.[3] The slope of the plot dEc/dt vs [Ly] can be taken as the calibration sensitivity, and for the condition without interfering species added, the estimated value was 4×10^{-5} nM^{-1} s^{-1} (Figure 3B). When 250 nM of CYT was added as interfering protein, the sensitivity did not change but the intercept with the ordinate axis was no longer ~0.0. The positive value of the intercept (~+0.011 V) indicates that some CYT adsorption is occurring because this protein is positive at neutral pH (pI = 10.5). The fact that the calibration sensitivity does not change in the presence of CYT, which was added inasmuch as 30% of the maximum concentration of Ly (840 nM), implies that the nonspecific adsorption of CYT does not compromise the specific sites for Ly and quantification is still viable at nanomolar levels even though the precision for some of the points in the curve is lower. When comparing the sensitivity of modified and pristine COC toward the adsorption of Ly, it is clear that COC-PEGA-PAA-anti-Ly has a sensitivity about 1 order of magnitude lower than pristine COC (3.9×10^{-4} nM^{-1} s^{-1}),[3] which shows that pristine COC has more adsorption sites precisely because of the indiscriminate nonspecific adsorption.[3] The dynamic range for

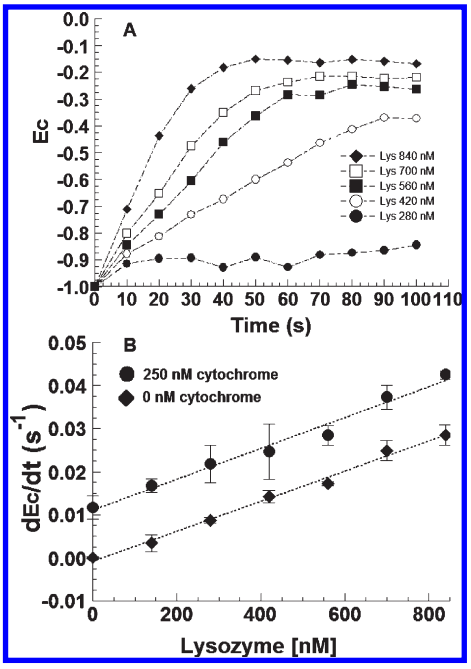

Figure 3. (A) Adsorption phase for different concentrations of Ly on COC-PEGA-PAA-anti-Ly microchannels. Ly solutions had pH 7.1 and 262 μS cm^{-1}. (B) Calibration curves for Ly and Ly spiked with 250 nM of CYT. Each curve containing seven calibration points was produced in the same COC-PEGMA-PAA-anti-Ly channel after recovery of the initial surface charge. Every point reported is the average of the dEc/dt magnitude for the first 30 s of the adsorption phase, obtained for the same concentration in three different microchannels. To recover the original surface after Ly adsorption, NaCl 0.5 M was flushed for 300 s. Dotted lines represent linear regression: $Y = 3.5 \times 10^{-5}X - 0.000\,82$ (r^2 = 0.992) for Ly and $Y = 2.9 \times 10^{-5}X + 0.011$ (r^2 = 0.990) for Ly(CYT).

Ly detection with COC-PEGA-PAA-anti-Ly is still in nanomolar concentrations, but the polyclonal antibodies provide some level of specificity. This result indicates that this method of monitoring the kinetics of adsorption by pulsed streaming potentials can be used to quantitatively measure analytes and their interactions with surface bound probes. For instance the equilibrium constant K_{eq} for the adsorption of Ly on COC-PEGA-PAA-anti-Ly was estimated to 2.7×10^6 M^{-1}. This value is about 1 order of magnitude lower than the K_{eq} value obtained for nonspecific adsorption of Ly directly on COC (3.6×10^7 M^{-1}),[3] which indicates that some of the binding strength is presumably traded off for the specificity that is gained. On the other hand, a K_{eq} value of 4.0×10^5 M^{-1} was found for the nonspecific adsorption of Ly on Au surfaces coated with citrate.[40] The fact of the matter is that the same type of intermolecular interactions that are responsible for specific binding are also involved in nonspecific adsorption; therefore, specificity does not guarantee a stronger interaction.

The COC-PEGA-PAA-anti-Ly surface showed good ability to recover the initial surface charge after 0.5 M NaCl was flowed during 300 s. In order to produce the calibration curves shown in Figure 3B, three microchannels were regenerated after Ly adsorption (Figure S6, Supporting Information). Each adsorption−regeneration cycle was repeated six times (one per each Ly concentration), and the recovery efficiency was expressed as % $R = (E_F/E_I) \times 100$, where E_I is the pulsed streaming potential of the surface before any Ly adsorption, measured with protein-free buffer, and E_F represents the signal with protein-free buffer after

dx.doi.org/10.1021/ac102769j |*Anal. Chem.* XXXX, XXX, 000–000

regeneration with NaCl. Figure S6 in the Supporting Information shows that the average % *R* per cycle is higher than 97% for each of the six Ly concentrations. This finding demonstrates that the COC-PEGA-PAA-anti-Ly composite surface is suitable for studying processes where renewal of the original surface is important, like kinetic studies of adsorption interactions with surface bound probes. Additional control experiments showed that in order to achieve these high levels of surface renewal, the presence of PEGA on the composite surface is needed. For instance, when a solution of Ly 320 nM was used for an adsorption−regeneration cycle on COC, the % *R* obtained was 60.9 ± 2.1, and in the case of COC-PAA, the % *R* was 84.6 ± 25.1.

CONCLUSIONS

We have demonstrated the inhibition of nonspecific adsorption of proteins after photografting of PEGA on COC microchannels. The nonionic and hydrophilic character of PEGA also substantially reduces the surface charge of pristine COC by decreasing the nonspecific adsorption of ions. Polyclonal antibodies with affinity for Ly were linked via amide bonds to carboxylate functionalities of PAA grafted on COC-PEGA. The quantification of Ly by pulsed streaming potentials in real time was attained with good linearity in the range 140−840 nM, even in the presence of 250 nM cytochrome as interfering species. The composite film COC-PEGA-PAA-anti-Ly showed a high renewability of the original surface charge after washing with a regeneration solution of NaCl. This regeneration allowed calibration at different concentrations of Ly on one single microchannel. The major result of this work is the development of a surface detection technique of general applicability with low cost and simple instrumentation. The approach does not require chemical labeling and provides significant mitigation of nonspecific adsorption while still providing nanomolar detection limits with some degree of specificity for Ly. It is envisioned that this kind of composite film in plastic microfluidics channels will provide an appropriate platform for further demonstration of the use of pulsed streaming potentials as a useful tool for studying protein−protein interactions in real time as well as the detection of bioprobes using affinity interactions.

ASSOCIATED CONTENT

Supporting Information. Additional experimental details plus data illustrating the characterization by AFM, ATR-FTIR, and pulsed streaming potentials during the preparation/optimization of the films. This material is available free of charge via the Internet at http://pubs.acs.org.

AUTHOR INFORMATION

Corresponding Author

*E-mail: jcalvarez2@vcu.edu.

ACKNOWLEDGMENT

The generous support of this work by the National Science Foundation through Grant CHE-0645494 is greatly appreciated.

REFERENCES

(1) Pu, Q.; Oyesanya, O.; Thompson, B.; Liu, S.; Alvarez, J. C. *Langmuir* **2007**, *23*, 1577–1583.
(2) Pu, Q.; Elazazy, M. S.; Alvarez, J. C. *Anal. Chem.* **2008**, *80*, 6532.
(3) Luna-Vera, F.; Alvarez, J. C. *Biosens. Bioelectron.* **2010**, *25*, 1539–1543.
(4) Hunter, R. J. *Zeta Potential in Colloid Science: Principles and Applications*; Academic Press: London, 1981; p 381.
(5) Chen, Y.-M.; Yu, C.-J.; Cheng, T.-L.; Tseng, W.-L. *Langmuir* **2008**, *24*, 3654–3660.
(6) Wegner, G. J.; Alastair, W. W.; Lee, J. L.; Codner, E.; Saeki, T.; Fang, S.; Corn, R. M. *Anal. Chem.* **2004**, *76*, 5677–5684.
(7) Bharadwaj, M.; Kohaar, I.; Hussain, S.; Tiwari, P.; Thakur, N.; Nasare, V.; Das, B. C.; Choundhury, S. R.; Sarkar, D. P. *Genomic Med.* **2008**, *2*, 273–283.
(8) Aguilar, M. I.; Small, D. H. *Neurotoxic. Res.* **2005**, *7*, 17–27.
(9) White, D. A.; Buell, A. K.; Dobson, C. M.; Welland, M. E.; Knowles, T. P. J. *FEBS Lett.* **2009**, *583*, 2587–2592.
(10) Lee, V. A.; Craig, R. G.; Filisko, F. E.; Zand, R. *J. Colloid Interface Sci.* **2005**, *288*, 6–13.
(11) Dang, F.; Hasegawa, T.; Biju, V.; Ishikawa, M.; Kaji, N.; Yasui, T.; Baba, Y. *Langmuir* **2009**, *25*, 9296–9301.
(12) Quinn, A.; Mantz, H.; Jacobs, K.; Bellon, M.; Santen, L. *EPL* **2008**, *81*, 56003.
(13) Lofas, S.; Johnsson, B. *J. Chem. Soc., Chem. Commun.* **1990**, 1526–1528.
(14) Zou, X. P.; Kang, E. T.; Neoh, K. G. *Plasmas Polym.* **2002**, *7*, 151–170.
(15) Iguerb, O.; Bertrand, P. *Surf. Interface Anal.* **2008**, *40*, 386–390.
(16) Zimmermann, R.; Norde, W.; Cohen Stuart, M. A.; Werner, C. *Langmuir* **2005**, *21*, 5108–5114.
(17) Dillon, P. P.; Killard, A. J.; Daly, S. J.; Leonard, P.; O'Kennedy, R. *J. Immunol. Methods* **2005**, *296*, 77–82.
(18) Tandon, V.; Bhagavatula, S. K.; Nelson, W. S.; Kirby, B. J. *Electrophoresis* **2008**, *29*, 1092–1101.
(19) Gupta, M. L.; Brunson, K.; Chakravorty, A.; Kurt, P.; Alvarez, J. C.; Luna-Vera, F.; Wynne, K. J. *Langmuir* **2010**, *26*, 9032–9039.
(20) Love, J. C.; Estroff, L. A.; Kriebel, J. K.; Nuzzo, R. G.; Whitesides, G. M. *Chem. Rev.* **2005**, *105*, 1103–1169.
(21) Uhlmann, P.; Merlitz, H.; Sommer, J. U.; Stamm, M. *Macromol. Rapid Commun.* **2009**, *30*, 732–740.
(22) Tsujii, Y.; Ohno, K.; Yamamoto, S.; Goto, A.; Fukuda, T. *Adv. Polym. Sci.* **2006**, *198*, 1–46.
(23) Zhao, B.; Brittain, J.; Zhou, W.; Cheng, S. Z. D. *J. Am. Chem. Soc.* **2000**, *122*, 2407–2408.
(24) Brittain, W. J.; Minko, S. *J. Polym. Sci., Part A: Polym. Chem.* **2007**, *45*, 3505–3512.
(25) Lin, H.; Van Wagner, E.; Swinnea, J. S.; Freeman, B. D.; Pas, S. J.; Hill, A. J.; Kalakkunnath, S; Kalika, D. S. *J. Membr. Sci.* **2006**, *276*, 145–161.
(26) Knoelle, W.; Scherzer, T.; Naumanov, S.; Mehnert, R. *Radiat. Phys. Chem.* **2003**, *67*, 341–345.
(27) Huang, L.; Li, Y.; Yang, J.; Zeng, Z.; Chen, Y. *Polymer* **2009**, *50*, 4325–4333.
(28) Gao, Z.; Henthorn, D. B.; Kim, C.-s. *J. Micromech. Microeng.* **2008**, *18* (045013), 7pp.
(29) Feng, L.; Zhou, S.; You, B.; Wu, L. *J. Appl. Polym. Sci.* **2007**, *103*, 1458–1465.
(30) Rajesh; Bisht, V.; Takashima, W.; Kaneto, K. *Biomaterials* **2005**, *26*, 3683–3690.
(31) Manning, G. S. *Polyelectrolytes*; Selegny, E., Mandel, M., Strauss, U. P., Eds. D. Reidel Publishing Company: Dordrecht, The Netherlands, 1974.
(32) Bohme, U.; Scheler, U. *Chem. Phys. Lett.* **2007**, *435*, 342–345.
(33) Schmitz, K. S. *Macroions in Solution and Colloidal Suspension*; VHC Publishers, Inc.: New York, 1993.
(34) Wright, A. K.; Thompson, M. R. *Biophys. J.* **1975**, *15*, 137–141.
(35) Grabarek, Z.; Gergely, J. *Anal. Biochem.* **1990**, *185*, 131–135.
(36) Bonanno, L. M.; DeLouise, L. A. *Langmuir* **2007**, *23*, 5817–5823.

(37) Xu, F.; Zhen, G.; Textor, M.; Knoll, W. *Biointerphase* **2006**, *1*, 73–81.
(38) Hodgkinson, G. N.; Hlady, V. *Croat. Chem. Acta* **2007**, *80*, 405–420.
(39) Arifuzzaman, S.; Ozcam, A. E.; Efimenko, K. *Biointherphases* **2009**, *4* (FA), 33–44.
(40) Glomm, R. W.; Halkkau, O.; Hanneseth, A. M. D.; Volden, S. *J. Phys. Chem. B* **2007**, *111*, 14329–14345.